

Response to reviewer #2:

We thank Reviewer #2 for his/her valuable and thoughtful comments. Our responses to the comments are provided below, with the reviewer's comments italicized and our responses in plain and bold fonts.

This paper presents a global modeling study on how aging due to ozone oxidation affects the lifetime, burdens, and concentrations of carbonaceous aerosols, with aging here defined as the conversion of carbonaceous from being hydrophobic to hydrophilic. This is a very important topic because accurately modeling this aging process is critical to predicting carbonaceous aerosol concentrations and determination of their health and climate impacts. While the topic is important and well within the scope of ACP, I have major concerns with this paper and do not recommend it for publication.

Major Comments

1. As noted by the other reviewer, this study considers only one of several aging mechanisms. This is a major weakness that renders the paper incomplete for publication in ACP. The only aging process considered in this study is the ozone oxidation of organic material coated on the carbonaceous aerosols. There are several issues with considering only this mechanism:

(a) The impact of this specific aging mechanism has already been studied using a global model by Tsigaridis and Kanakidou (2003). In fact, this study used the exact formulation as Tsigaridis and Kanakidou (2003) (based on the chamber study of Pöschl et al., (2001)); therefore, the implementation of this mechanism and implications discussed in Section 3.2 are not new.

(b) Among all the processes by which carbonaceous aerosols are aged in the atmosphere, oxidation by ozone is not even the most important. The processes by which carbonaceous aerosols are aged are summarized nicely in section 5 of Kanakidou et al., (2005). At the minimum, this study needs to consider aging by condensation of H₂SO₄ and coagulation, which are more important in polluted regions.

Response :

We have expanded our work and made significant revision to our manuscript. First, in addition to the chemical oxidation aging scheme, now we have also included the condensation-coagulation aging as well as the combined aging schemes in GEOS-Chem. These different aging effects have been compared with each other through sensitivity model simulations. We would also like to point out that, one major point of our study is to evaluate the potential effects of these updated aging schemes on the long-range/intercontinental transport of carbonaceous aerosols which was not done in previous studies.

We have added text for the condensation-coagulation aging scheme as follows.

Section 1 Introduction-“In addition, physical processes, such as condensation and coagulation, also make important contributions to the aging of aerosols. The aging of soot particles by these processes at a polluted region is simulated by Riemer et al. (2004), with condensation of sulfuric acid onto the surface of soot particles dominant during daytime while coagulation being an important process during nighttime. The e-folding aging lifetimes are approximate 8 h below 250 m during day time, with 2 h between 250 m and 3000 m. During nighttime, the aging timescale was found to be 10-40 h on average. These aging time scales are further employed by Croft et al. (2005) in a global model to estimate the global lifetime and burden of BC. However, the parameterization for this scheme tends to strongly depend on the regional case that was chosen by Riemer et al. (2004), which is not appropriate for global model parameterization and thus could result in larger uncertainties at GCM scales. By contrast, Liu et al. (2011) proposed a new condensation-coagulation scheme to globally simulate the aging rate of BC by assuming it is proportional to the gas concentration of sulfuric acid that are produced from the oxidation of SO₂ by hydroxyl radicals (OH) in the ambient air. As a result, the lifetime of BC in the model is predicted to be temporally and spatially variable, which improved the model performance in terms of comparisons to surface observations as well as aircraft campaigns.”

Section 1 Introduction-“We also follow Liu et al. (2011) to account for the condensation-coagulation aging effects.”

Section 2 Approach and model descriptions-“Following Liu et al. (2011), condensation-coagulation aging scheme is also investigated. The condensation of sulfuric acid gas onto the surface of particles leads to the conversion of carbonaceous aerosols from hydrophobic to hydrophilic. The conversion rate of particles by condensation is proportional to the sulfuric acid gas concentration, which is

$$k_{CC} = (D_g M / \rho R \delta_c) \cdot [H_2SO_4]_g, \quad (3)$$

where k_{CC} is the rate coefficient for condensation-coagulation aging scheme; subscript of CC represents condensation-coagulation; $[H_2SO_4]_g$ is the gas concentration of H₂SO₄ in the air; D_g is the diffusivity of H₂SO₄ in the atmosphere; M and ρ are the molecular weight and particle-phase density of H₂SO₄; R is the mass median radius of hydrophobic carbonaceous aerosols; δ_c is the equivalent coating thickness for the carbonaceous aerosols to take the critical soluble mass into account).

The reaction of SO₂ with OH produces H₂SO₄ in the air. The steady state concentration of H₂SO₄ in the air is derived as

$$[H_2SO_4]_g = \frac{k_1 [OH] [SO_2]}{\sum_i 4\pi D_g r_i}, \quad (4)$$

where k_1 is the reaction rate coefficient for $\text{SO}_2 + \text{OH}$; $[\text{OH}]$ and $[\text{SO}_2]$ are gas concentrations of hydroxyl radicals and sulfur dioxide in the ambient air; i represents each particle in the air and r_i is the particle radius; $\sum_i r_i$ is the sum of all particle radius in each grid box. Combining Eqs. (3) and (4), we have

$$k_{CC} = \beta \cdot [\text{OH}] \left(\text{where } \beta = \frac{k_1 M [\text{SO}_2]}{\sum_i 4\pi R \delta_c r_i} \right), \quad (5)$$

Taking coagulation effect into account, Eq. (5) becomes

$$k_{CC} = \beta \cdot [\text{OH}] + \alpha, \quad (6)$$

where β and α are assumed to be constant, with values $4.6 \times 10^{-12} \text{ cm}^3 \text{ molecule}^{-1} \text{ s}^{-1}$ and $5.8 \times 10^{-7} \text{ s}^{-1}$. With globally average concentration of OH is about $10^6 \text{ molecules cm}^{-3}$, β is derived by assuming an e-folding aging time of 2.5 days; α is estimated by assuming e-folding lifetime for coagulation is 20 days.

With Eq. (6), we obtain

$$\tau_{CC} = \frac{1}{\beta \cdot [\text{OH}] + \alpha}, \quad (7)$$

where τ_{CC} is the e-folding conversion lifetime from condensation-coagulation scheme.”

Section 3.2-“3.2 Impacts of the condensation-coagulation aging mechanism on model simulations of carbonaceous aerosol

The τ values by condensation-coagulation aging scheme strongly depend on the global distributions of OH concentrations. Due to the low surface concentrations of OH in the Arctic and Antarctic, compared with the oxidation aging scheme, hot spots for τ values shift from tropical regions to both Poles (Fig. 8), which is consistent with the findings by Liu et al. (2011). However, both aging schemes have long τ values at the Amazon regions, South Asia and West Africa. Moreover, τ values at the northern midlatitude also significantly increase by more than a factor of 4, implying lower aging rates for primary carbonaceous aerosols from the anthropogenic emissions and more hydrophobic aerosols existing in the atmosphere. Figure 9 shows the vertical profile of τ values with highest ones located at the upper troposphere, indicating lowest OH concentrations there. Overall, this aging scheme leads to the global average burden (0.146 Tg) and lifetime (7.29 days) of BC increase by 25%, compared with the control simulation (Table 1). The global average burden of OC is 0.607 Tg, with lifetime 5.18 days, which increases by 13% by contrast with the control runs. As discussed in Section 3.1, the oxidation aging scheme increases the burdens and lifetimes of BC and OC, compared with the condensation-coagulation aging scheme, implying lower aging efficiency.

With the condensation-coagulation aging scheme, model simulated surface BC concentrations are shown in Figure 10. Compared with the control run, increases BC concentrations are observed over South America, South Africa, Southeastern Asia and high latitude of North Hemisphere, by up to $0.05 \mu\text{g C m}^{-3}$. Ratio plot shows that this aging scheme increases the BC surface concentrations at both Poles by over a factor of 2. Similar

impacts are found for model simulated OC concentrations in surface air, with largest increases by up to $0.25 \mu\text{g C m}^{-3}$ over South America, South Africa and South Asia (Figure 11). Ratio plot shows that OC surface concentrations at remote regions increase by a factor of 1.7.

Global vertical profiles of BC and OC are shown in Figure 12 and 13, respectively. It reflects that the concentrations of BC and OC at the Arctic regions are significantly strengthened, which means that the burdens of carbonaceous aerosols in the Arctic is larger than the control runs and the magnitude of the impact of anthropogenic emissions from lower latitude on the Arctic is larger, compared with the control runs. This is justified by global models, which always underestimate the carbonaceous aerosols against aircraft campaigns as well as long-term surface observations (Chung and Seinfeld, 2002; Heald et al., 2011; Wang et al. 2011; Liu et al. 2011). Similar to the oxidation aging scheme, OC concentrations at the tropical regions are strengthened due to strong emissions of biomass burning as well as biogenic emissions there. Strongest perturbations to simulated BC and OC are found at the Arctic and Antarctic regions as well as upper troposphere by a factor of 2-4.”

We have also added text for the combined aging scheme as follows.

Section 1 Introduction-“Finally, a combined aging scheme accounting for both the chemical oxidation and physical processes is applied in the model.”

Section 2 Approach and model descriptions-“To consider the combined aging effects from oxidation and condensation-coagulation, we define the aging factor for oxidation as

$$f_{OXD} = \frac{\tau_{OXD}}{\tau_0}, \quad (8)$$

where τ_0 is the global uniform a priori lifetime (1.15) days used in GEOS-Chem. Similarly the aging factor for condensation-coagulation is defined as

$$f_{CC} = \frac{\tau_{CC}}{\tau_0}, \quad (9)$$

The overall lifetime accounting for both the oxidation and condensation-coagulation effects is

$$\tau_{OCC} = \tau_0 * f_{OXD} * f_{CC}, \quad (10)$$

Eq. (10) can be rewritten as

$$\tau_{OCC} = \frac{\tau_{OXD} * \tau_{CC}}{\tau_0}, \quad (11)$$

Thus,

$$k_{OCC} = \frac{1}{\tau_{OCC}} = k_{OXD} * k_{CC} * \tau_0, \quad (12)$$

where k_{OCC} is the rate coefficient for the combined aging scheme.”

Section 3.3-“The combined aging scheme used in the sensitivity test is based on the competition effect from both chemical and physical aging. Croft et al. (2005) have simply

summed up the rate coefficients from oxidation and condensation-coagulation aging schemes, which results in poor model performance against observations at source regions. With the combined aging scheme, global burdens of BC and OC (0.178 Tg for BC and 0.693 Tg for OC) are found to be the largest and higher than the control simulation by 52% and 29%, with longest global average BC and OC lifetimes 8.86 days and 5.91 days, respectively (Table 1). BC and OC lifetimes and burdens are calculated to be on the high end, compared with model simulations (i.e. Liu et al. 2011; Colarco et al. 2010; Koch et al. 2009 and Pierece et al. 2007), except OC burden (Table 1).

Compared with the control runs, surface concentrations of BC and OC at source regions significantly increase by up to $0.175 \mu\text{g C m}^{-3}$ and $0.734 \mu\text{g C m}^{-3}$, respectively, with largest perturbation to remote regions by a factor of 4 (Figs. 14 and 15). Figures 16 and 17 show the combined aging scheme increases global distributions of model simulated BC and OC at lower troposphere by up to $0.019 \mu\text{g C m}^{-3}$ and $0.069 \mu\text{g C m}^{-3}$. Additionally, model simulated BC and OC concentrations at upper troposphere are more than a factor of 2 than the control runs.”

(c) The aging process implemented in this study is based on ozone oxidation of benzo[a]pyrene coated on carbonaceous aerosols. Benzo[a]pyrene is not representative of organic material on carbonaceous aerosols. The implication of this should be discussed.

Response :

We have added discussion in the text -

“There are very limited experimental data available on the aging of carbonaceous aerosols and the chamber results (Pöschl et al., 2001) used for chemical aging in this study are most representative for BC, but not necessarily for OC. The strong sensitivities of the model simulations of carbonaceous aerosols to the aging schemes indicate that further studies on the aging carbonaceous aerosol are needed to better understand the effects of carbonaceous aerosol on climate, atmospheric composition and air quality.”

2. I also agree with the other reviewer that comparison to observations at two marine sites is absolutely inadequate. There is no reason provided why those two sites were chosen over the other sites. As the authors noted, the two sites evaluated are implicated by marine carbonaceous aerosol– so why not chose sites where marine carbonaceous aerosol is not a concern? The evaluation should not be limited to IMPROVE sites but should include other surface measurements outside of the US. Furthermore, since significant differences are found above the surface layer between the updated and the control runs, a comparison of modeled vs. observed

vertical distribution is needed. There are data from field projects, e.g., ACE-Asia, that can be used for such comparison.

Response :

We have done an more extensive model evaluation using observational data from multiple datasets including ground-based Interagency Monitoring of Protected Visual Environments (IMPROVE) data (<http://views.cira.colostate.edu/web/>), surface observations from China Atmosphere Watch Network (CAWNET) in 2006 (Zhang et al., 2008) and BC/OC campaign during 2002-2003 in Europe by the European Monitoring and Evaluation Programme (EMEP) (<http://www.nilu.no/projects/ccc/emepdata.html>). Additionally, we use aircraft campaign, Asian Pacific Regional Aerosol Characterization Experiment (ACE-Asia) in 2001, to compare with the vertical distributions of model calculated carbonaceous aerosols by the updated aging schemes.

We have added the text-

“3.4 Comparison with observations

Ground-based Interagency Monitoring of Protected Visual Environments (IMPROVE) observational data in 2005 (<http://views.cira.colostate.edu/web/>), surface observations from China Atmosphere Watch Network (CAWNET) in 2006 (Zhang et al., 2008) and BC/OC campaign during 2002-2003 in Europe by the European Monitoring and Evaluation Programme (EMEP) (<http://www.nilu.no/projects/ccc/emepdata.html>) are employed to evaluate the global carbonaceous aerosol simulation results from the control run and updated aging scheme simulations. Additionally, we use aircraft campaign, Asian Pacific Regional Aerosol Characterization Experiment (ACE-Asia) in 2001, to compare with the vertical distributions of model calculated carbonaceous aerosols by the above aging schemes. For the purpose of comparison to measurements, we treat BC equivalent to EC in this study although different measurement techniques, such as thermal technique for EC and photo-absorption for BC, could sometimes result in significant mass concentration differences (Jeong et al., 2004). Observational sites from these three observational networks are shown in Figure 22. We use the annual mean data for BC and OC in 2005 to compare with observations by assuming that the interannual variability is small.

Surface concentrations of BC and OC from models and selected sites of IMPROVE are shown in Figure 23a and 23b. Annual mean BC and OC from control simulations are generally underestimated by a factor of 2, which are consistent with other model findings (Park et al., 2003; Liu et al., 2011). With the updated aging schemes, model simulated BC and OC improve the underestimate within a factor of 1.5. The comparisons of BC surface concentrations against observations from EMEP are shown in Figure 23a. Model generally

captures well BC concentrations, except four sites located at Italy, Belgium, Portugal and Great Britain. Without these four sites, our updated aging schemes, especially the combined and TRIPLE aging schemes, almost bring model simulated BC equals to observations. By contrast, the control simulation largely underestimates OC (more than 6 times), even the updated aging schemes only slightly improve the model performance within a factor of 6 (Figure 23b). This can be explained that open fire emissions are probably underestimated by the model emission inventory because open fires are the dominant source of OC. The scenario is even worse at the CAWNET of China. The control simulation significantly underestimates BC and OC by a factor of 7 and 16, respectively (Figs. 23a and 23b). This is mainly due to the underestimates of anthropogenic emissions and seasonal fire activities in South Asia (Wang et al. 2011). Wang et al. (2011) doubled the anthropogenic emissions in Asia but still get low bias of model simulated BC, compared with CAWNET observations. This implies that the anthropogenic emission sources in China should more than double.

Model simulated BC and OC concentrations in surface air at three remote sites are compared with the observational data from IMPROVE network: the Hawaii Volcanoes National Park (HAVO) (19.4°N, 155.3°W), the Haleakala National Park (HALE) (20.8°N, 156.3°W) and Denali National Park (DENALI) (63.7°N, 149°W). All the values are annual means for 2005. Compared to the control run, the simulation with oxidation aging scheme increases the annual mean concentration of BC and OC at HAVO by approximately 38% and 30%, respectively (Figs. 23a and 23b). The TRIPLE aging scheme performs the best, followed by the combined aging scheme, increasing BC and OC by 80% and 59%, 60% and 48% respectively, compared with the control run. This considerably improves the model performance, although it still underestimates the observations by a factor 2. Identifying the sources for the remaining model underestimates of carbonaceous aerosols is beyond the scope of this study, but it has been reported that there are around 10% of sea salt aerosols containing organic compounds during the First Aerosol Characterization Experiment (ACE 1) by analyzing the composition of marine particles under various environmental conditions (Middlebrook et al., 1998). Cavalli et al. (2004) reported even higher fraction of organic compounds in marine aerosols during phytoplankton bloom period at North Atlantic, with 54% and 4% of organic compounds in marine aerosols under submicron and supermicron modes, respectively. Global models estimate that the marine OC emission source is around 8-9 Tg C yr⁻¹ (Meskhidze et al., 2011; Spracklen et al., 2008), which is further confirmed by ship campaigns (9 Tg C yr⁻¹) reported by Lapina et al. (2011).

In an attempt to compare the model simulated vertical profiles of BC and OC with observations, aircraft campaign ACE-Asia during spring 2001 is employed to compare with our model simulations (Huebert et al., 2004). With the TRIPLE aging scheme, model simulated BC and OC are observed to increase by ~64% and ~45% in 4-6 km altitude, compared with the control run (Figure 24). By contrast, model simulated BC and OC by

the oxidation aging scheme are found to increase by ~15% and ~13% at the same altitude range, with similar results for the condensation-coagulation and combined aging schemes. However, the updated aging schemes only slightly improve the model performance by a few percent below 4 km altitude. Due to missing a large amount of BC and OC sources in the free troposphere that originate from Asia emissions, model simulations significantly underestimate BC and OC by a factor of 10-100 (Heald et al., 2005). In particular, an important source of secondary organic aerosols that is produced in Asia source regions transports to the free troposphere of Pacific Ocean that GEOS-Chem doesn't capture, which leads to large model bias against observations."

Other Comments

1. Line 2, Page 28999: *"This significantly [emphasis mine] improves..."* The use of "significantly" overestimates the improvement because the improvement is much smaller than the difference between the updated model results and observations.

Response :

We have changed "significantly" to "considerably".

2. Line 21, Page 28999: *"_ in surface air ... (Table 1)." "Surface air" here is a typo. The values reported in Table 1 are global average lifetimes, including contributions from above the surface layer.*

Response :

Point well taken. The global average value of τ in surface air refers to the conversion lifetimes from hydrophobic to hydrophilic for carbonaceous aerosols averaged globally for the 1st model layer (which is different from the global average lifetime in Table 1). We have removed the quotation of "Table 1" in this sentence.

3. Page 28997, around equations (1) and (2): *The text should mention that this is the same formulation implemented in Tsigaridis and Kanakidou (2003).*

Response :

We have added the text before equation (1) and rewritten the sentence as

“With the same scheme as used by Tsigaridis and Kanakidou (2003), we implemented in GEOS-Chem the experiment-based formulation for the turn-over rate from hydrophobic to hydrophilic is:”

References

Tsigaridis, K. and Kanakidou, M.: Global modelling of secondary organic aerosol in the troposphere: a sensitivity analysis, Atmos. Chem. Phys., 3(5), 1849–1869, doi:10.5194/acp-3-1849-2003, 2003.

Kanakidou, M., Seinfeld, J. H., Pandis, S. N., Barnes, I., Dentener, F. J., Facchini, M. C., Van Dingenen, R., Ervens, B., Nenes, A., Nielsen, C. J., Swietlicki, E., et al.: Organic aerosol and global climate modelling: a review, Atmos. Chem. Phys., 5(4), 1053–1123, doi:10.5194/acp-5-1053-2005, 2005.

Pöschl, U., Letzel, T., Schauer, C. and Niessner, R.: Interaction of ozone and water vapor with spark discharge soot aerosol particles coated with benzo[a]pyrene: $\hat{A}^{\sim}L^{\prime}$ O₃ and H₂O adsorption, benzo[a]pyrene degradation, and atmospheric implications, J. Phys. Chem. A, 105(16), 4029–4041, doi:10.1021/jp004137n, 2001.

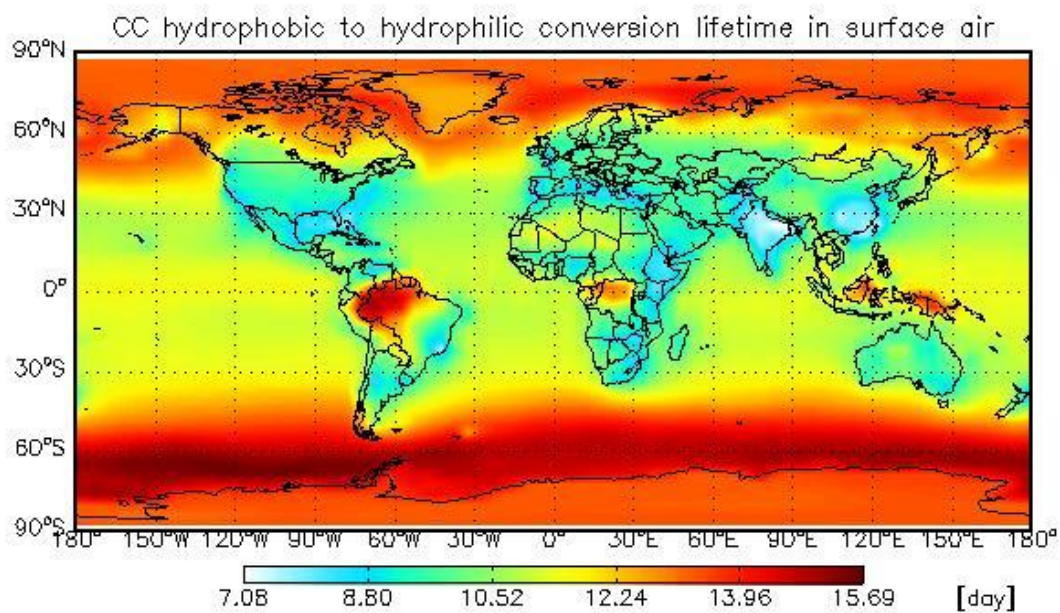


Fig. 8. Model calculated hydrophobic to hydrophilic conversion lifetime for carbonaceous aerosols in surface air by condensation-coagulation aging scheme. CC (hereinafter) represents condensation-coagulation aging scheme.

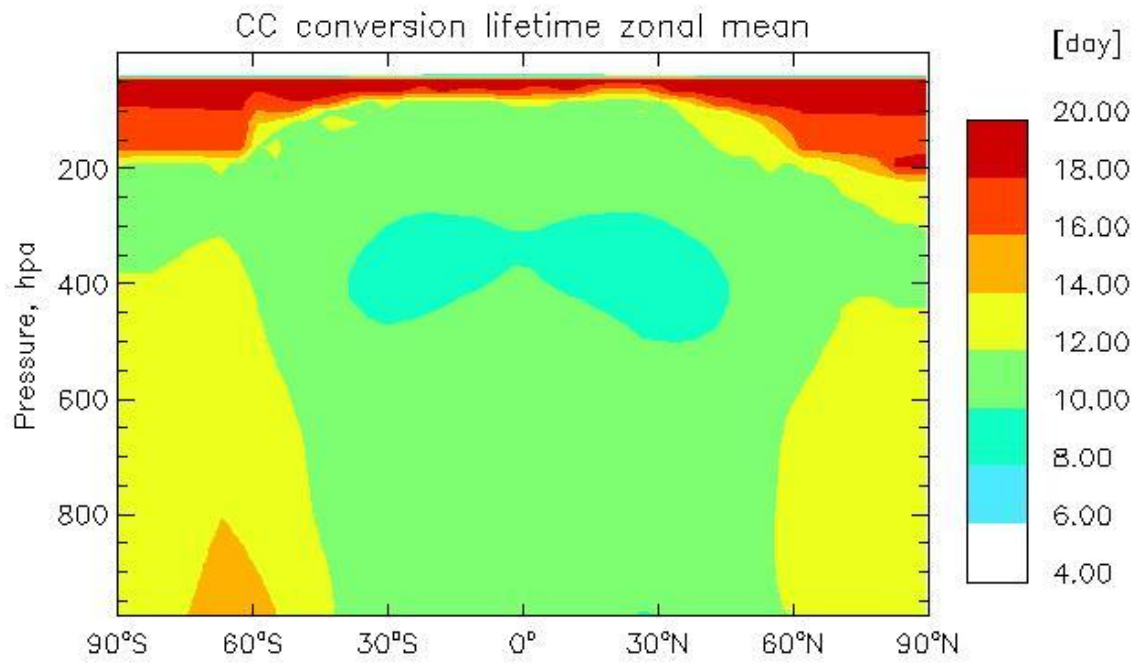


Fig. 9. Zonal mean plot for hydrophobic to hydrophilic conversion lifetime for carbonaceous aerosol by condensation-coagulation aging scheme.

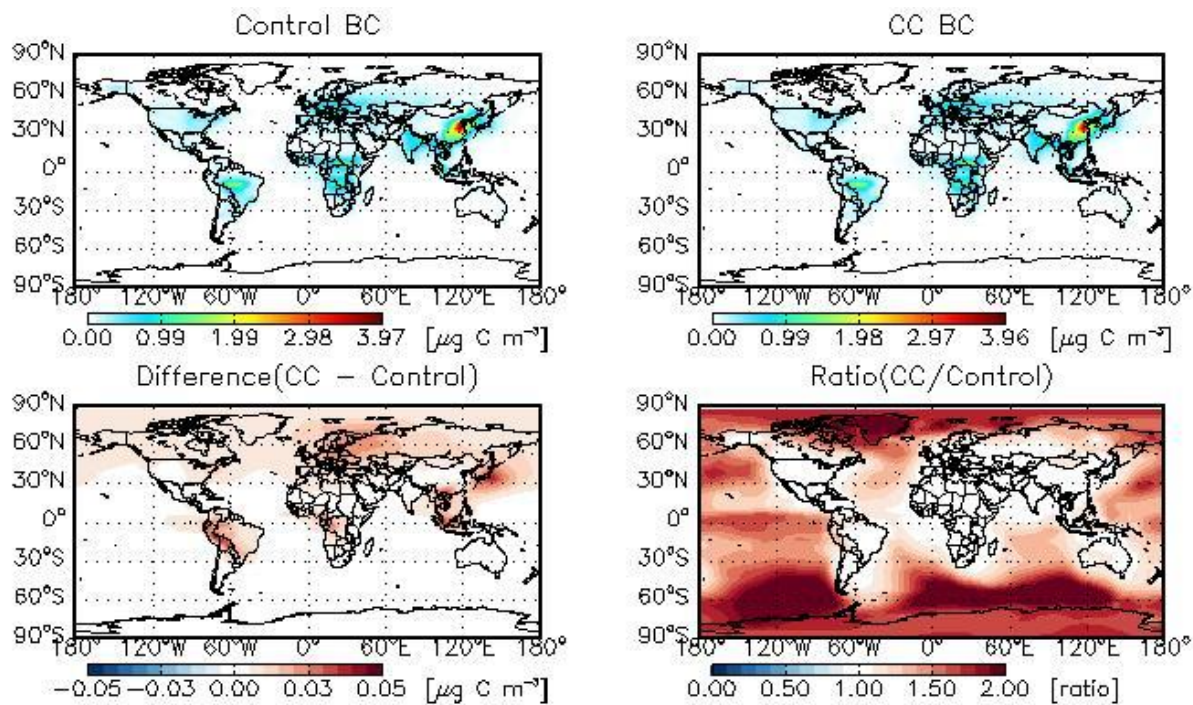


Fig. 10. Model simulated annual mean surface BC concentrations from the sensitivity run versus the control run. (Upper left) BC concentrations from the control run; (upper right) BC concentrations from the sensitivity run using the condensation-coagulation aging scheme; (lower left) differences between the sensitivity run and control run results; (lower right) ratio between sensitivity run and control run results.

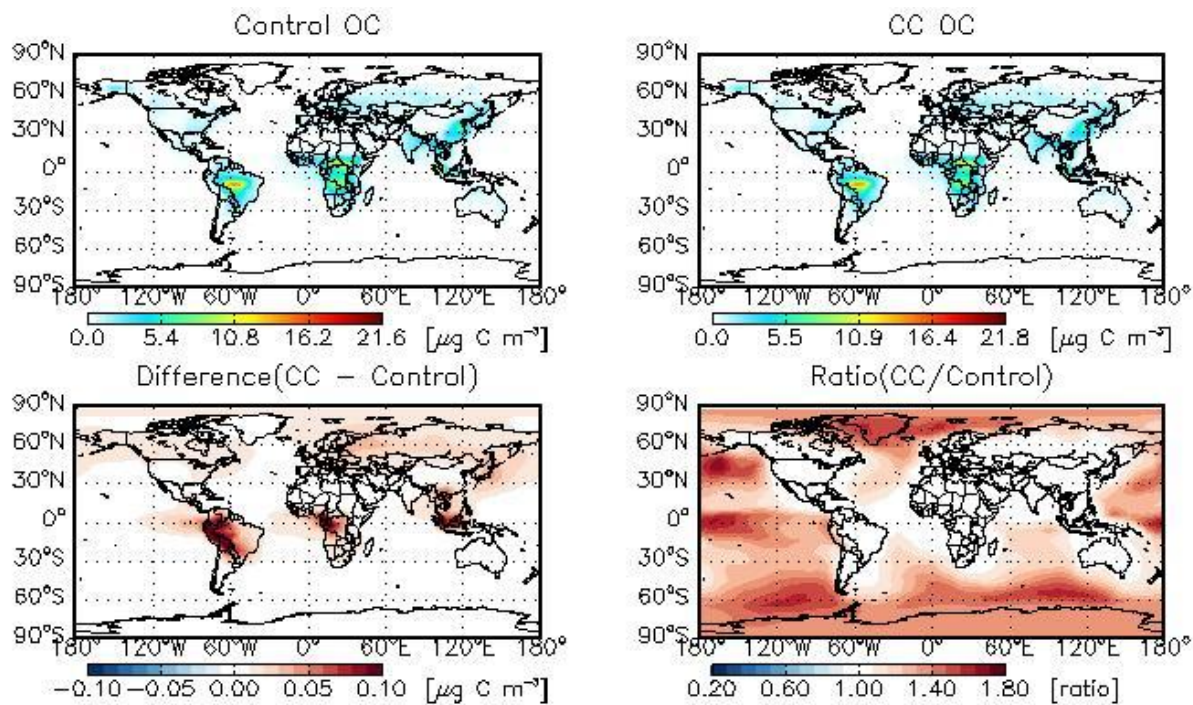


Fig. 11. Same as Figure 10 but for OC.

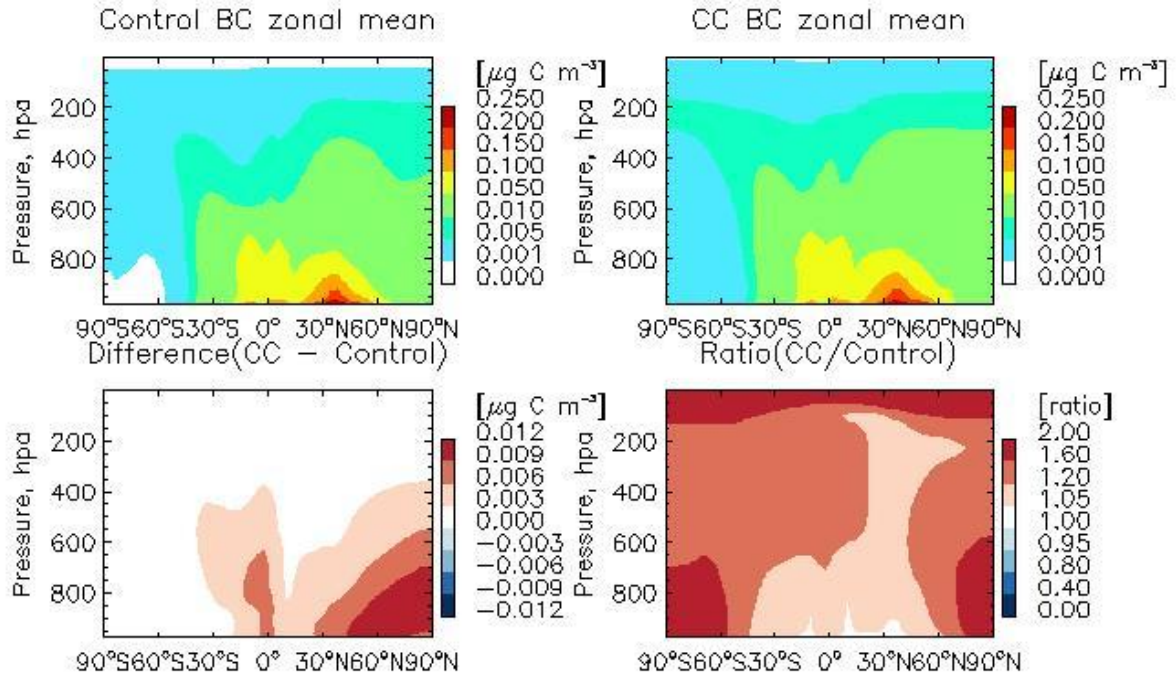


Fig. 12. Same as Figure 10 but for zonal mean.

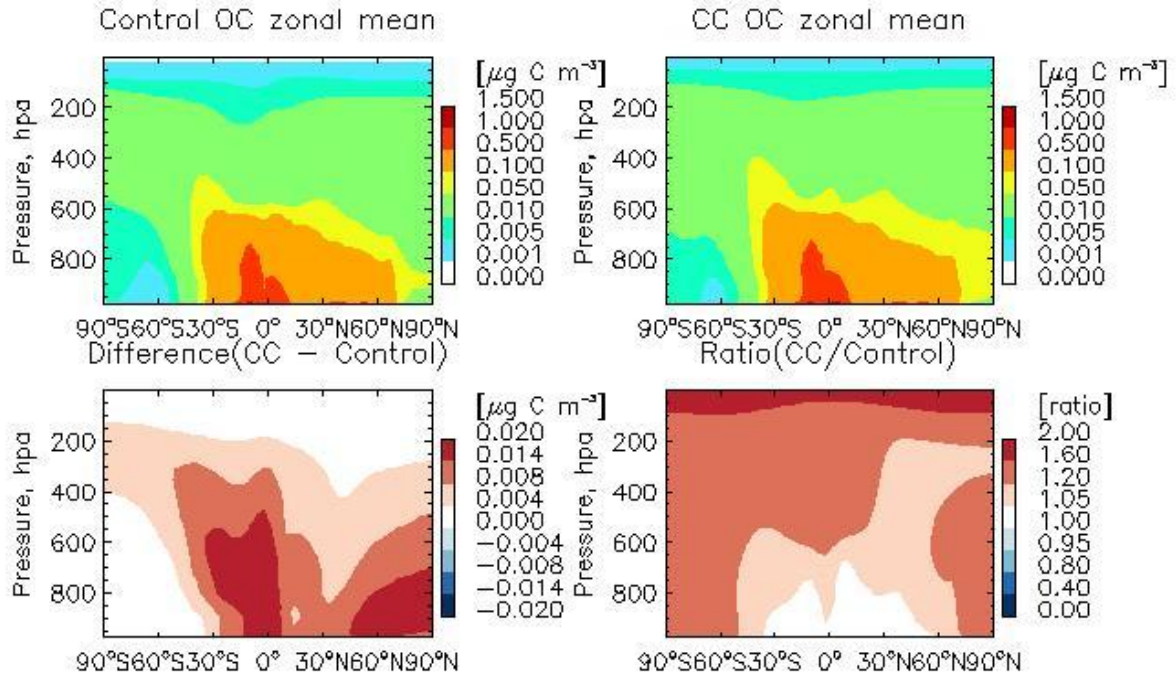


Fig. 13. Same as Figure 11 but for zonal mean.

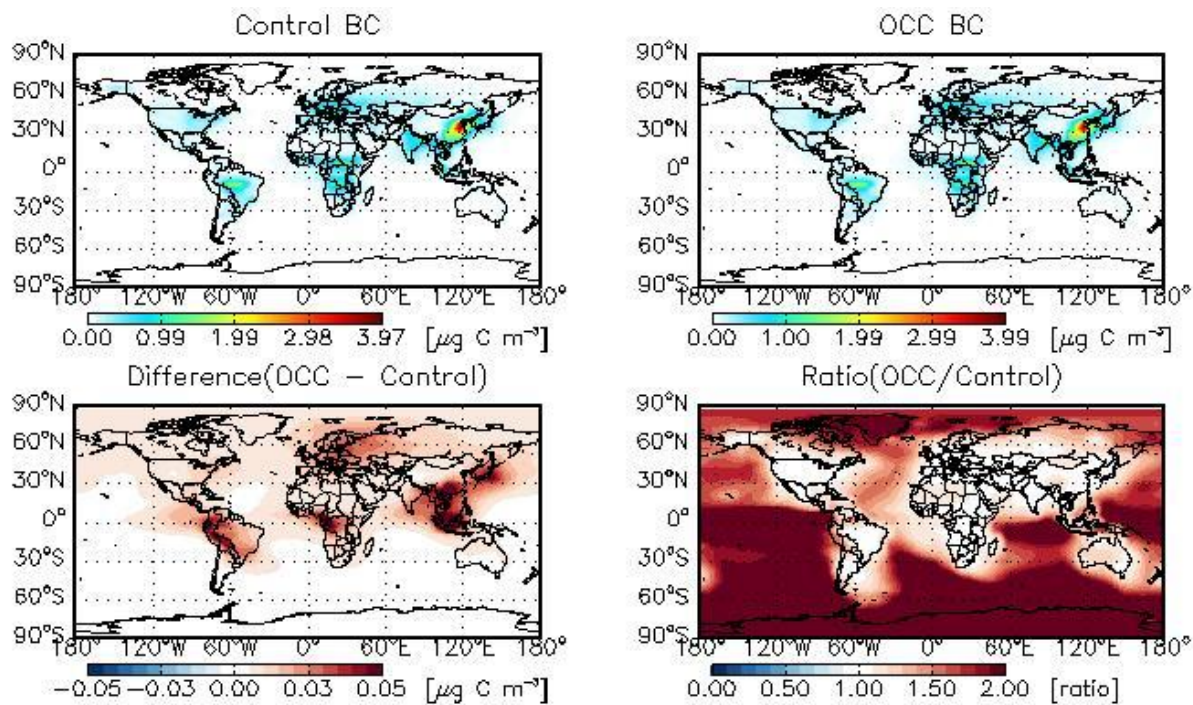


Fig. 14. Model simulated annual mean surface BC concentrations from the sensitivity run versus the control run. (Upper left) BC concentrations from the control run; (upper right) BC concentrations from the sensitivity run using the combined aging scheme; (lower left) differences between the sensitivity run and control run results; (lower right) ratio between sensitivity run and control run results. OCC (hereinafter) represents the combined aging scheme.

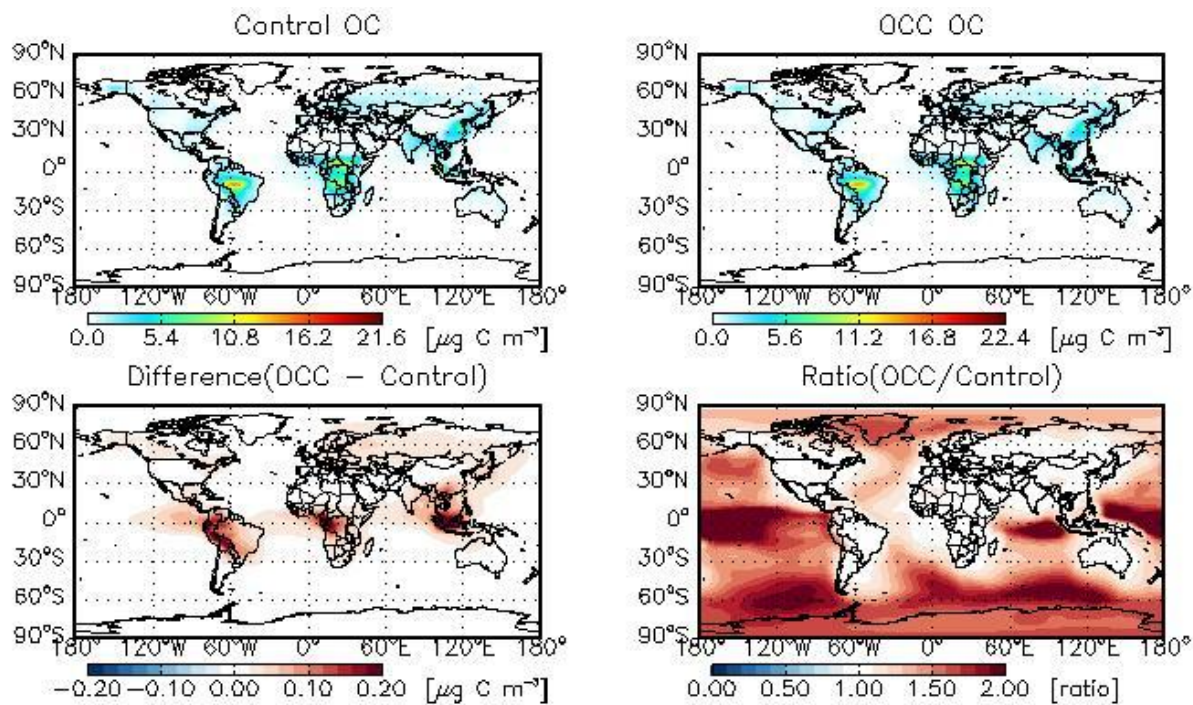


Fig. 15. Same as Figure 14 but for OC.

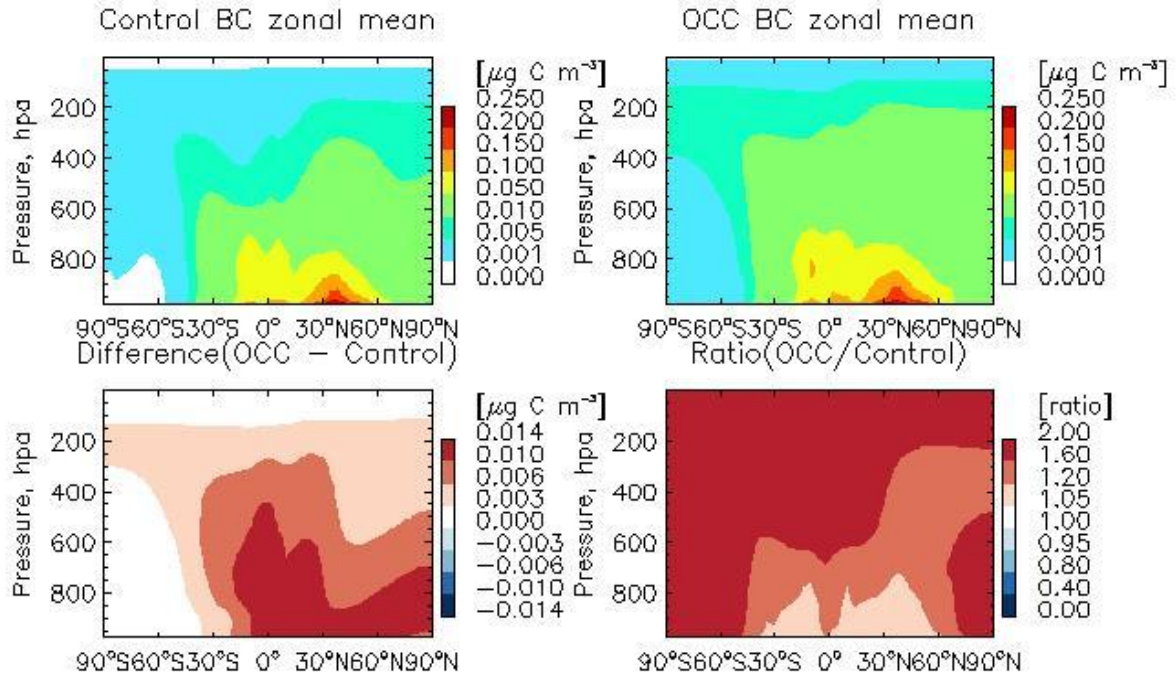


Fig. 16. Same as Figure 14 but for zonal mean.

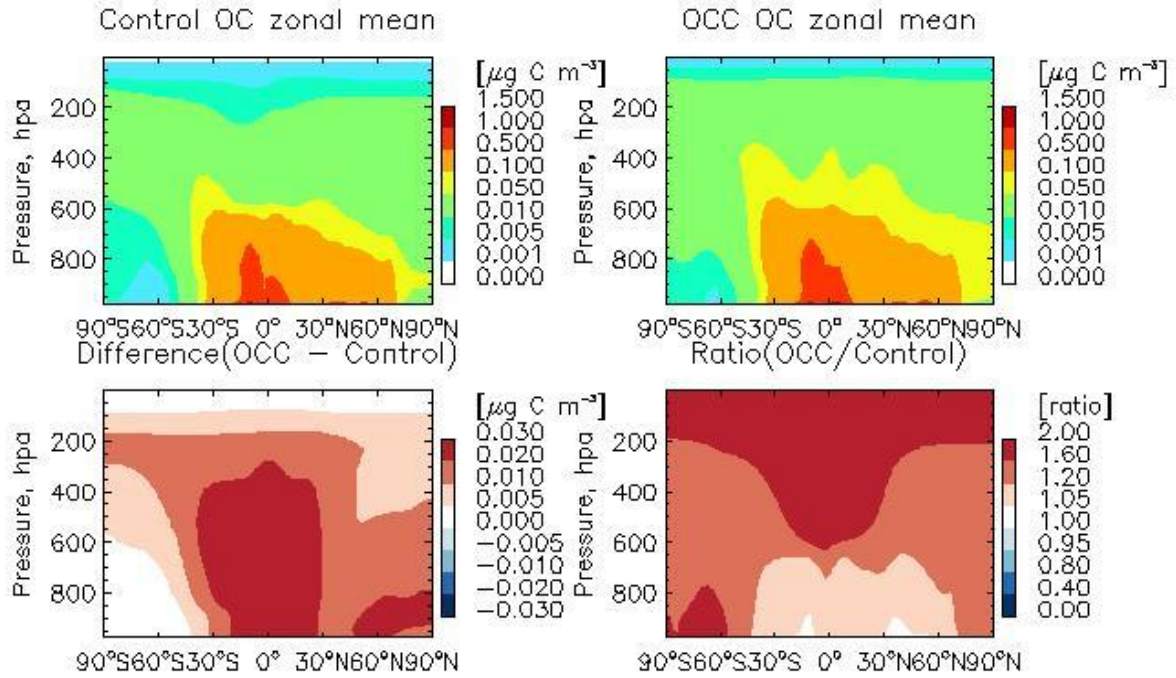


Fig. 17. Same as Figure 15 but for zonal mean.

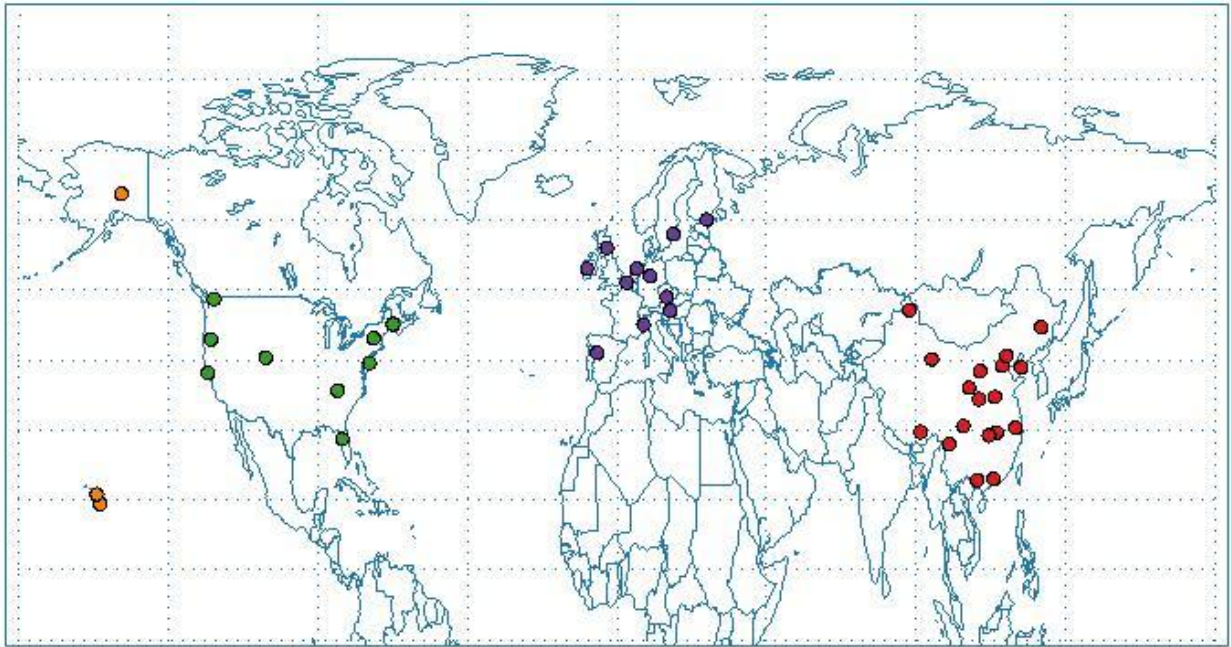


Fig. 22. Observational sites from CAWNET (red circles), EMEP (purple circles) and IMPROVE (green circles). Remote sites-HAVO, HALE and DENALI are from IMPROVE with orange circles.

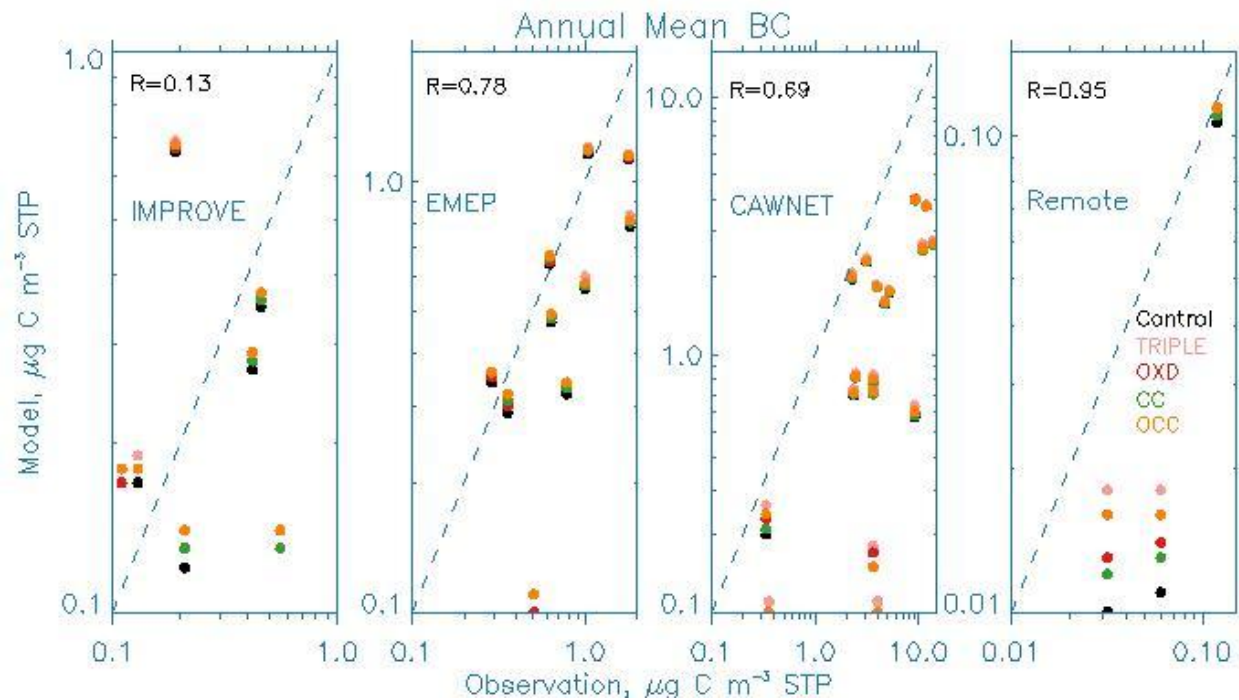


Fig. 23a. Scatter plots for annual mean BC between model simulation results and observations from IMPROVE, EMEP, CAWNET and remote sites. Black circles represent control simulation results, with TRIPLE, oxidation, condensation-coagulation and combined aging schemes are shown by purple, red, green and orange circles, respectively.

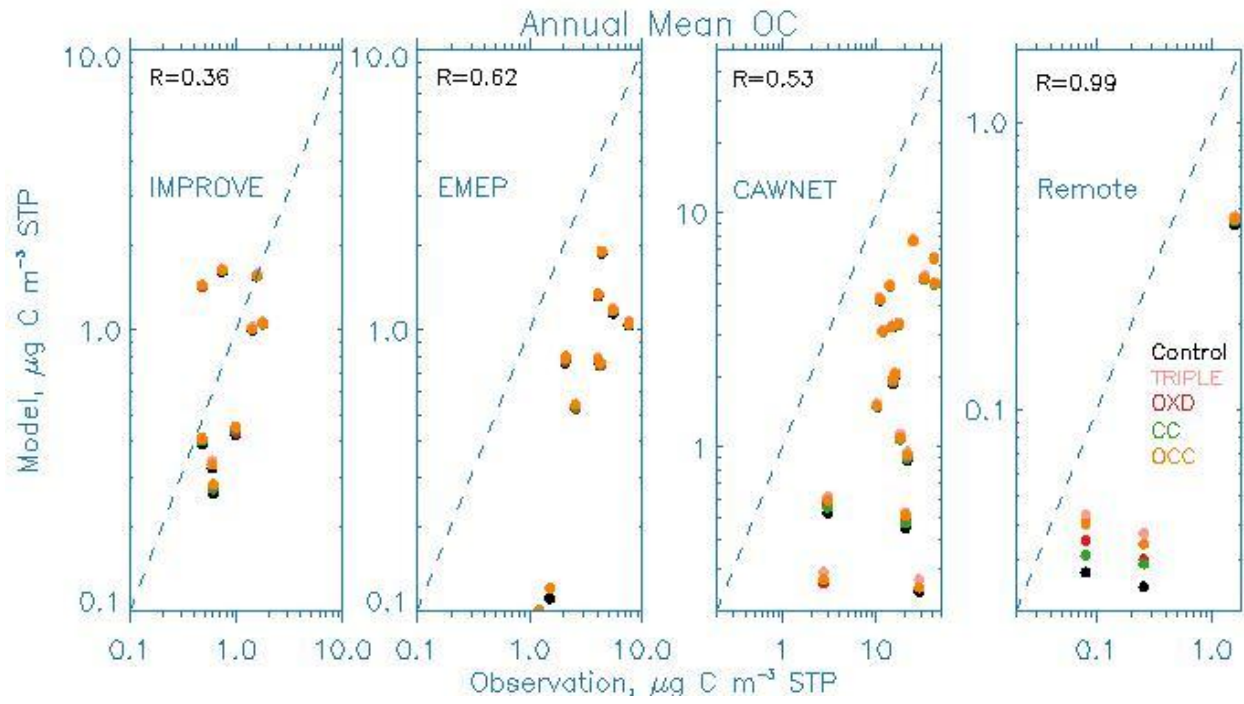


Fig. 23b. Same as Figure 23a but for OC.

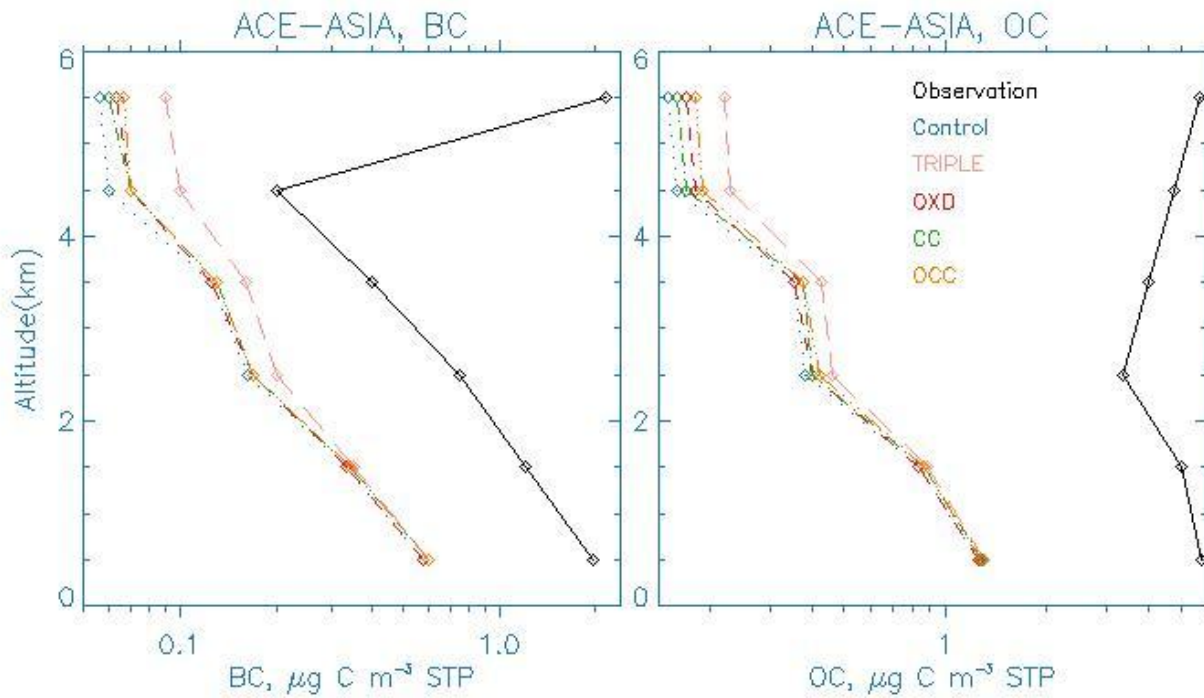


Fig. 24. Vertical profiles of BC (left) and OC (right) between model simulations from various aging schemes and NSF/NCAR C-130 aircraft campaign in ACE-Asia. Model and observational data are averaged over 1-km altitude bins. Simulation data is sampled along the track of C-130 during April 2001.